

# OBSERVATIONS OF MODE COUPLING IN THE SOLAR CORONA AND BIPOLAR NOISE STORMS

S. M. WHITE, G. THEJAPPA\*, and M. R. KUNDU

*Astronomy Program, University of Maryland, College Park, MD 20742, U.S.A.*

(Received 13 April, 1991; in revised form 19 August, 1991)

**Abstract.** We review high-spatial-resolution observations of the Sun which reflect on the role of mode coupling in the solar corona, and present a number of new observations. We show that typically polarization inversion is seen at 5 GHz in active region sources near the solar limb, but not at 1.5 GHz. Although this is apparently in contradiction to the simplest form of mode coupling theory, in fact it remains consistent with current models for the active region emission. Microwave bursts show no strong evidence for polarization inversion. We discuss bipolar noise storm continuum emission in some detail, utilizing recent VLA observations at 327 MHz. We show that bipolar sources are common at 327 MHz. Further, the trailing component of the bipole is frequently stronger than the leading component, in apparent conflict with the 'leading-spot' hypothesis. The observations indicate that at 327 MHz mode coupling is apparently strong at all mode-coupling layers in the solar corona. The 327 MHz observations require a much weaker magnetic field strength in the solar corona to explain this result than did earlier lower-frequency observations: maximum fields are 0.2 G. This is a much weaker field than is consistent with current coronal models.

## 1. Introduction

Polarization is one of the fundamental diagnostics of radio astronomy, and particularly of solar radio astronomy. Since we can predict the polarization properties of the common radiation emission mechanisms (free-free, gyroresonance, synchrotron, plasma emission, and cyclotron maser emission), polarization data can be used to determine magnetic field strengths and directions in regions where no other information on the magnetic field is available. However, the interpretation of the polarization of solar radio emission is not always straightforward. One of the reasons is that the apparent polarization of radio emission can change as the emission propagates from the source to us. The effects of mode coupling in the corona are responsible: the removal of linear polarization by Faraday depolarization is a well-known example of the possible effects.

The theory of mode coupling in cold plasmas has been studied in considerable detail specifically with reference to solar observations (Piddington and Minnett, 1951; Cohen, 1960; Melrose, 1973, 1974a, b, 1980a; Zheleznyakov, 1977; Zheleznyakov and Zlotnik, 1978, 1988; Suzuki and Sheridan, 1980; Bandiera, 1982). There are two electromagnetic modes which can propagate in a cold plasma: the ordinary ( $o$ ) and extraordinary ( $x$ ). In general these wave modes are elliptically polarized, and they propagate independently. In the limit of a near-vacuum, which applies to the medium in which they are detected on Earth, both are circularly polarized. If there is no coupling between the two modes during propagation they will remain in their original modes upon arrival at Earth.

\* On leave from the Indian Institute for Astrophysics, Bangalore, India.

Then the local sense of circular polarization would tell us directly the identification of the mode as it was in the source. Any linear polarization originally present is wiped out because the two modes have different dispersive properties: the information on linear polarization is contained in the relative phase between the two components, but at different frequencies this phase rotates at different rates and is not preserved over a finite receiver bandwidth.

In general we expect that there is coupling between the modes which may permit them to retain their sense of circular polarization as they propagate, rather than their mode identity. This is known as 'strong' coupling. In this case the observed sense of circular polarization at Earth tells us the sense of circular polarization in the source, and this is useful since if we already know the mode of emission we can deduce the orientation of the magnetic field in the source.

The purpose of this paper is to review recent results relevant to the study of mode coupling in the corona. There has been relatively little attention paid to this topic since the 1970's, and we feel that it is valuable particularly to discuss the information which the contemporary observations by synthesis telescopes such as the Very Large Array and the Westerbork Synthesis Radio Telescope have provided in recent years. Many of these observations have been carried out with higher spatial resolution than was available for earlier discussions. In particular, we will provide multi-frequency observations showing clearly the frequency at which mode coupling occurs above an active region, present VLA observations of bipolar noise storms at 327 MHz, and discuss the presence of mode coupling during flares. We will first summarize the predictions of the theory of mode coupling as a framework for further discussion.

## 2. Predictions of Mode Coupling Theory

We summarize the discussions by Zheleznyakov (1977) and Melrose (1980). The magnetoionic modes in a cold plasma are circularly polarized provided that

$$u = \frac{f_B f}{2(f^2 - f_p^2)} \frac{\sin^2 \theta}{\cos \theta} \ll 1 \quad (1)$$

(quasi-circular limit), where  $f$  is the frequency,  $f_B$  the gyrofrequency,  $f_p$  the plasma frequency, and  $\theta$  is the angle between the wave vector and the magnetic field. In the limit  $f \gg f_p$ ,  $f_B$  the inequality (1) holds everywhere except in a small range of angles near  $\theta = \pi/2$ . In the opposite limit (quasi-planar) the two modes are linearly polarized.

The parameter which describes coupling between the two modes in general has no simple form, but in order of magnitude it is

$$Q \approx \begin{cases} \frac{cf}{f_p^2 L} & \text{quasi-circular,} \\ \frac{cf^4}{f_p^2 f_B^3 L} & \text{quasi-planar,} \end{cases} \quad (2)$$

where  $L^{-1}$  is a typical gradient; in the quasi-planar limit  $L^{-1}$  is the gradient in the angle  $\theta$ . In the lower corona we expect that  $L \approx 10^8$  cm, increasing to  $10^9$ – $10^{10}$  cm in the middle and upper corona; values of  $L$  may be smaller where inhomogeneities occur. The quasi-circular limit of  $Q$  describes coupling across a region where the modes remain circularly-polarized, but the refractive index changes. The form of  $Q$  for the quasi-planar limit actually refers to coupling across the boundary between a region where the modes are circularly polarized and a region where they are linearly polarized. Regions where the modes are linearly polarized are generally thin because they only occur for a narrow range of the angle  $\theta$ . Note that in the quasi-planar limit  $Q \approx (f/f_i)^4$  with

$$f_i, \text{ GHz} \approx 0.5 \left( \frac{n_e}{10^9 \text{ cm}^{-3}} \right)^{1/4} \left( \frac{L}{10^9 \text{ cm}} \right)^{1/4} B_{\text{gauss}}^{3/4}. \quad (3)$$

Thus there exists a critical frequency,  $f_i$ , which typically lies in the range of observed radio frequencies, 100 MHz–10 GHz, at which coupling passes sharply from strong at high frequencies to weak at low frequencies. Below this frequency we expect to see polarization reversals (e.g., in the case of active region emission, the sense of polarization does not correspond to the  $x$ -mode in the source). Note that  $f_i$  depends only weakly on the plasma density and scale length in the QT layer, but strongly on the magnetic field strength.

The importance of (1) is that in the quasi-circular limit  $Q \ll 1$  for virtually all plausible conditions in the solar corona. Thus as radiation propagates where the natural modes are circularly polarized it retains its mode identity ('weak' coupling). It follows that the sense of circular polarization (left- or right-hand rotation) will also remain unchanged until it reaches a point where the component of  $\mathbf{B}$  along the line of sight changes sign. At this point either  $\mathbf{B} = 0$ , or else  $\theta \approx \pi/2$ . In the latter case we call it a 'quasi-transverse' or QT layer, and then  $u \gg 1$ . In the quasi-transverse case the natural modes are linearly polarized, and the polarization and mode resulting when the wave re-emerges into a quasi-circular region depends on the value of  $Q$  in the QT layer. If the radiation encounters one QT layer along the line of sight where  $Q \ll 1$  (weak coupling), then its sense of circular polarization will be reversed with respect to the sense in the source. If it encounters an even number of weak-coupling QT layers its final sense of circular polarization will remain as it was originally.

In the conventional model (Piddington and Minnett, 1951; Bandiera, 1982), radiation from the limbward part of a bipolar active region near the limb will encounter one more QT layer in the active region itself which radiation from the nearest part of the active region does not encounter, and if this is a weak coupling QT layer then the limbward radiation suffers a polarization reversal and both limbward and diskward parts of the active region arrive with the same polarization (outside the active region, lines of sight to both diskward and limbward parts of the active region are likely to encounter the same QT regions).

Thus a basic prediction of mode coupling theory is that there should exist some critical frequency,  $f_i$ , depending on parameters in the active region, such that for  $f > f_i$  polarization reversal of limbward sources is not observed, whereas for  $f < f_i$  it is observed.

This conclusion can be altered by several effects. Firstly, for emission near the plasma frequency, important at metric wavelengths, refraction must be taken into account: refraction tends to make radiation propagate parallel to the refractive index gradient, and thus away from QT regions (Melrose, 1973). A consequence is that the apparent sources (or height) of the radiation will be shifted relative to the true source, and it can then encounter a QT layer in which  $f_i$  is lower than it would have been for the original line of sight, improving the chances for strong coupling.

Secondly, radiation may encounter current sheets in the corona in which the magnetic field is zero. Melrose (1973) suggested this in order to achieve low magnetic fields within the QT region, but Zheleznyakov and Zlotnik (1978, 1988) pointed out that in the limit  $B = 0$  the mode-coupling theory described above is no longer pertinent, because in this case the two radiation modes become degenerate. The degenerate modes will support any incident polarization and allow it to propagate across the  $B = 0$  layer, preserving the polarization when it emerges on the other side. Thus the  $B = 0$  layer acts like a strong-coupling layer, in the sense that the polarization (linear, circular, or elliptical) is preserved. Zheleznyakov and Zlotnik (1988) note that in most cases radiation will encounter a  $B = 0$  layer inside a region which is quasi-circular, and thus the radiation retains its initial sense of circular polarization as it propagates through the layer.

Occasionally a line of sight may intersect a  $B = 0$  layer inside a QT region. Zheleznyakov and Zlotnik (1988) discuss the case in which coupling from the quasi-circular region into the QT region is weak at both ends of the QT region (typical coronal parameters for solar metric emission suggest that this will be the case). Thus as the radiation couples into the linearly-polarized natural modes in the QT layer, the mode identity is preserved. Then the important question is whether coupling is weak or strong as the radiation passes from the QT region into and out of the  $B = 0$  layer. If coupling is weak then the result is preservation of the original sense of polarization of the radiation when it re-emerges into a region where the natural modes are circularly polarized, because effectively the radiation passes through two weak-coupling QT layers with a strong-coupling  $B = 0$  layer in between. Conversely, strong coupling as the radiation passes from the QT region to the  $B = 0$  layer can result in emerging radiation which has suffered a reversal of circular polarization, because the linear polarization acquired when it first enters the QT region is retained until it emerges back into the quasi-circular region on the other side of the layer. Preservation of the plane of linear polarization is equivalent to retention of mode identity (this is what happens in a single weak-coupling QT layer without  $B = 0$ ), and then the radiation mode is preserved as it passes back into the quasi-circular region with weak coupling. The coupling parameter describing coupling from the QT region into the  $B = 0$  layer is  $Q = cf/f_p^2 L \cos^2 \theta$ , where now  $L^{-1}$  is the gradient in magnetic field strength in the coupling layer (Zheleznyakov, Kocharovskii, and Kocharovskii, 1984). Zheleznyakov and Zlotnik (1988) show that one expects that all coronal QT layers such that  $B = 0$  inside are likely to be weak-coupling, and they will preserve the sense of circular polarization.

We note that if radiation is strongly coupled from the quasi-circular region into the QT region initially then we return to the usual case: strong coupling from the QT region

to the  $B = 0$  layer produces preservation of circular polarization, while weak coupling there produces polarization inversion (preservation of mode identity).

Depolarization due to mode coupling has been inferred from observations of low polarization in fundamental plasma emission, and is attributed to the conversion of circular to linear polarization in a layer with  $Q \approx 1$  (Zheleznyakov and Zlotnik, 1964), with the subsequent loss of the linear polarization by Faraday rotation. We will not discuss this further here.

### 3. Mode Coupling and the Microwave $S$ Component

The microwave  $S$  component, or slowly-varying component (SVC), is that component of the Sun's emission associated with active regions. The character of SVC emission is a strong function of frequency. In the frequency range 5–10 GHz it tends to be dominated by highly-polarized, high-brightness-temperature cores (Kundu, 1959) which are attributed to thermal gyroresonance emission (Ginzburg and Zheleznyakov, 1961; Zheleznyakov, 1962; Kakinuma and Swarup, 1962). Bipolar active regions may show several such cores. There is also a low-brightness-temperature, low-polarization extended component which is attributed to thermal bremsstrahlung by dense coronal plasma. At higher frequencies (e.g., the VLA frequency of 15 GHz) the coronal magnetic fields are generally not strong enough to produce significant gyroresonance emission, although occasionally this is seen (Abramov-Maksimov and Gelfreikh, 1983; White, Kundu, and Gopalswamy, 1991b), and SVC is dominated by the thermal bremsstrahlung component. At lower frequencies (e.g., the VLA frequency of 1.5 GHz) thermal bremsstrahlung by the hot, high, dense loops seen to emit soft X-rays becomes optically thick, and tends to obscure any gyroresonance from lower in the corona.

The observations of SVC show that limb regions often contain polarization reversal for the limbward components at 5–7 GHz (e.g., Peterova and Akhmedov, 1974; Kundu *et al.*, 1977; Kundu and Alissandrakis, 1984; Alissandrakis and Kundu, 1984), but that at 1.5 GHz both limb and disk regions seem to be bipolar (Dulk and Gary, 1983; Bastian, 1987; Gopalswamy, White, and Kundu, 1991). No clear conclusion can be reached at the VLA observing frequency of 15 GHz, for lack of suitable observations.

To illustrate the conclusion that 5 GHz SVC often shows reversal while 1.5 GHz does not, in Figure 1 we present VLA observations of a limb region (AR 5148 on 1990 September 13) at 1.5 and 4.8 GHz. The data were taken when the VLA was in 'D' configuration. They thus have low spatial resolution, but demonstrate the effects of mode coupling well. The region on this day consisted of two spots: the leading spot has positive magnetic polarity while the trailing spot has negative magnetic polarity. At 5 GHz there are strong sources with coronal brightness temperatures ( $1.0 \times 10^6$  K) over both spots, but the emission from both parts of the active region has a positive  $V$  flux, which corresponds to a polarization in the sense of the  $x$ -mode in the leading part of the active region. At 1.5 GHz we see only a single source covering both spots, probably unresolved, at a coronal temperature ( $1.4 \times 10^6$  K). However, the  $V$  map at 1.5 GHz shows that the  $V$  flux reverses sign between the leading and trailing parts of the region,

so that both correspond to  $x$ -mode emission in the source. The 0.33 GHz observation, to be discussed below, shows a bipolar noise storm over this active region with the two components having opposite polarization from the two components of the 1.5 GHz  $V$  map, consistent with emission being in the  $o$ -mode at 0.33 GHz.

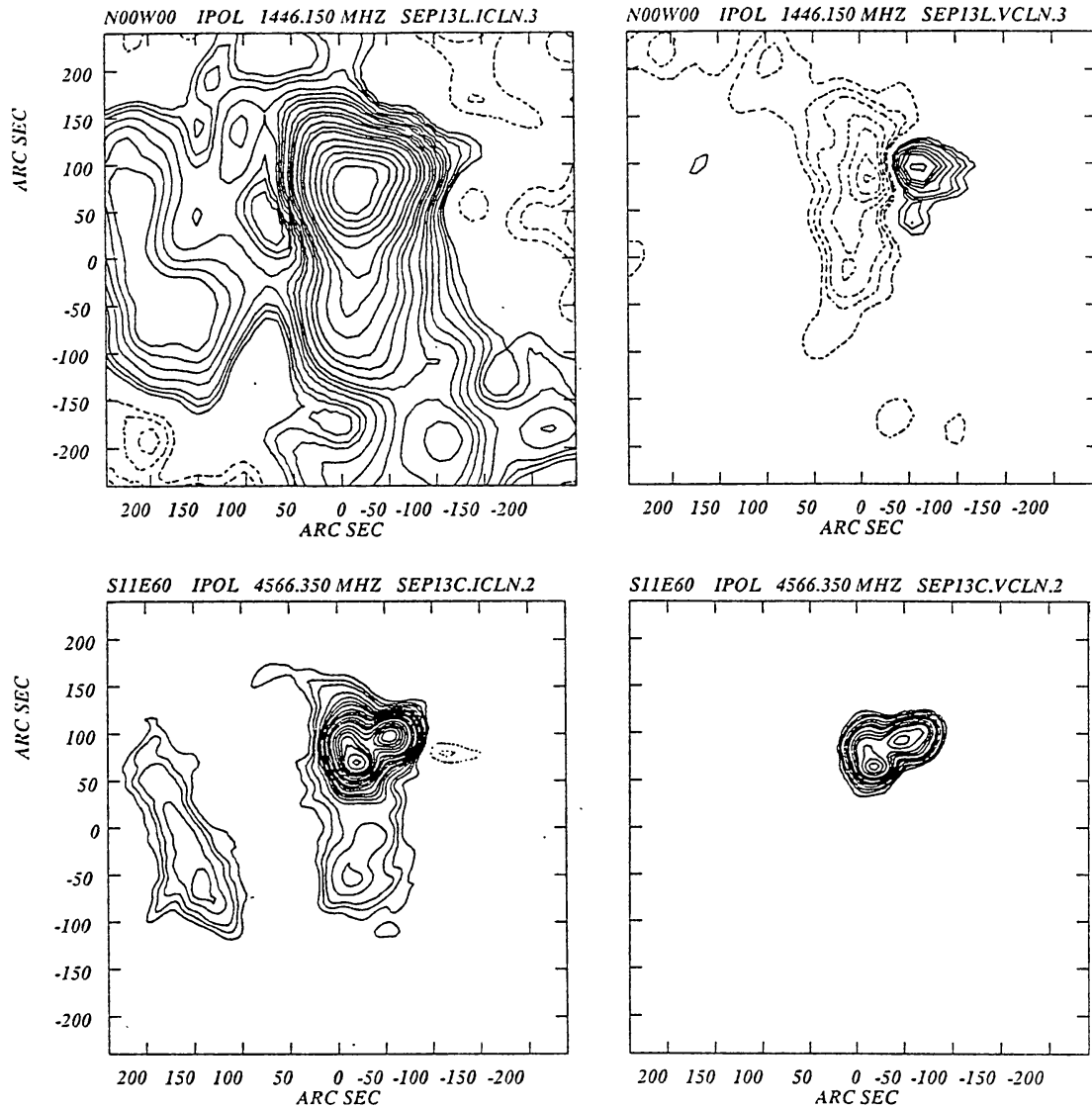


Fig. 1. 1.5 GHz (upper two panels) and 5 GHz (lower two panels) VLA 'D' configuration observations of an active region (AR 5148) on 1988 September 13. The left-hand panels are plots of total intensity, while the right hand maps are contour plots of the circularly polarized flux (Stokes  $V$ ), in units of degrees Kelvin brightness temperature. This figure illustrates the fact that polarization reversal is seen in the 5 GHz polarized emission from the limbward portion of the active region (the two peaks in the 5 GHz  $V$  map lie over sunspots of opposite magnetic polarity), but not in the 1.5 GHz emission (the  $V$  map shows oppositely polarized sources). The source at the left-hand edge of the two total intensity panels is emission from coronal material above the east limb. The 1.5 GHz maps have been corrected for the primary beam response, and this makes the noise level somewhat higher than usual. The contour level in the 1.5 GHz maps is  $10^4$  K, while that in the 5 GHz maps is 5000 K, with contours at the following multiples of the contour interval: -12, -10, -8, -6, -4, -3, -2, 2, 3, 4, 6, 8, 10, 12, 16, 20, 24, 32, 40, 48, 64, 80, 96, 112, 160, 192, and 224. The peak brightness temperature is  $1.45 \times 10^6$  K at 1.5 GHz and  $1.02 \times 10^6$  K at 5 GHz. Peak brightness temperatures in the  $V$  maps are  $-1.25 \times 10^5$  K at 1.5 GHz and  $+2.63 \times 10^5$  K at 5 GHz. The restoring beam size was  $44'' \times 41''$  at 1.5 GHz and  $22'' \times 15''$  at 5 GHz.

This same pattern was seen on 1988 September 11 and 1988 September 12, when the region was closer to the east limb. However, on 1988 September 17, when the region was near disk center, the 1.5 and 0.33 GHz maps show the bipolar pattern but now the 5 GHz map (discussed in White, Kundu, and Gopalswamy, 1991a) shows the trailing part of the region to have a negative  $V$  flux, rather than a positive  $V$  flux as it had in Figure 1.

The result that 5 GHz observations show polarization reversal at the limb while 1.5 GHz observations do not is clearly in contradiction to the predictions of the simple mode-coupling theory of the previous section, which says that all frequencies below some critical frequency  $f_t$  should show reversal while all frequencies above  $f_t$  should not. However, we need to take into account the fact that  $f_t$  for lines of sight at 1.5 GHz probably differs from  $f_t$  for lines of sight at 5 GHz. (In effect the model of Suzuki and Sheridan (1980) incorporates this result, and they indeed find that the region of strong coupling is larger at low frequencies than at high frequencies). The value of  $f_t$  is most sensitive to the magnetic field strength, and the magnetic field in the QT layer along the line of sight at a given frequency is probably related to the strength of the field in the source. As many authors have argued, the highly polarized component at 5 GHz is due to gyroresonance emission from regions of 600 G magnetic field strength, relatively low in the corona. On the other hand 1.5 GHz emission is thought to be optically thick due to the thermal opacity of the dense loops over active regions visible in soft X-rays. Thus for lines of sight at 1.5 GHz, the values of  $n_e$ ,  $B$ , and  $L^{-1}$  encountered in the QT layer in the active region will tend to be much lower than for the line of sight at 5 GHz. Typical values of  $B$  in the polarized 1.5 GHz sources are 20 G (Dulk and Gary, 1983; Gopalswamy, White, and Kundu, 1991), and so we expect that  $B$  in the QT layer for 1.5 GHz is at least an order of magnitude below that at 5 GHz. It is also an order of magnitude lower than would be the case if the 1.5 GHz radiation were gyroresonance emission, when  $B = 200$  G in the source. Thus the polarization observations at 1.5 GHz may be indirect evidence that 1.5 GHz emission is thermal bremsstrahlung.

For example, if we take  $n_e = 10^9 \text{ cm}^{-3}$ ,  $B = 100$  G, and  $L = 10^9$  cm in the 5 GHz QT layer, we find  $f_t = 16$  GHz and  $f < f_t$  as required. On the other hand if  $n_e = 10^8 \text{ cm}^{-3}$ ,  $B = 5$  G, and  $L = 2 \times 10^9$  cm in the 1.5 GHz QT layer, then  $f_t = 1.1$  GHz and  $f > f_t$  as required by the observations. We note that  $f_t$  is most sensitive to  $B$ , and thus the lack of reversal at 1.5 GHz is equivalent to an upper limit on  $B$  in the QT layer. Note also that Peterova and Akhmedov (1974) find that reversal is seen at 3.3 GHz.

Thus the high resolution interferometer observations of polarization are consistent with the current models for SVC. The observational result at 15 GHz is not clear, and difficult to predict: again, gyroresonance emission is likely to encounter the QT layer with a field much higher than in the 5 GHz QT layer, and this may result in polarization reversal being seen there also.

We also note that in general magnetic fields at a given height in the corona are thought to be larger in the leading than in the trailing portion of an active region, since generally photospheric data indicate stronger fields in the leading spot. This asymmetry should be seen as an eastern-hemisphere/western-hemisphere asymmetry: lines of sight to limb-

ward sources on the east limb encounter stronger fields in QT layers than comparable lines of sight on the west limb, so that polarization reversal should be seen to higher frequencies on the east limb than on the west, and also seen closer to central meridian passage in the east than in the west. This latter effect is apparently seen (Peterova and Akhmedov, 1974; Kundu and Alissandrakis, 1984); also, the fact that reversal occurs closer to CMP at higher frequencies (Peterova and Akhmedov, 1974) is consistent with geometric considerations (Bandiera, 1982).

#### 4. Mode Coupling and Solar Microwave Bursts

Even less attention has been paid to mode coupling in solar microwave bursts than in SVC. Early interest focussed on the observed reversal of polarization of burst emission as a function of frequency (Tanaka and Kakinuma, 1959; Zheleznyakov and Zlotnik, 1964), and this continues to be mentioned as an example of mode coupling (Melrose, 1980a; Alissandrakis, 1986; Zheleznyakov and Zlotnik, 1988). However, the reversal of polarization with frequency can also be interpreted as confirmation of the nonthermal gyrosynchrotron model for solar microwave bursts: in this model the optically thin, high-frequency emission should be polarized in the sense of the  $x$ -mode, but the optically thick, low-frequency emission should be weakly in the sense of the  $o$ -mode, which has a higher effective brightness temperature than the  $x$ -mode (due to the fact that the  $o$ -mode must resonate with higher-energy electrons at a given frequency in order to achieve optically-thick emission: Ramaty, 1969). An alternative explanation is that any thermal absorption process acting on nonthermal gyrosynchrotron emission will preferentially absorb the  $x$ -mode, leaving the radiation polarized in the sense of the  $o$ -mode (Preka-Papadema and Alissandrakis, 1988); in addition, below about 1.5 GHz plasma emission may also be contributing to the  $o$ -mode polarization of flare radiation. Alissandrakis and Preka-Papadema (1984) discuss mode-coupling in their models of flaring coronal loops.

Here we will try to compare mode-coupling evidence in burst observations with active region indicators. Before doing so, we point out the difficulties in such a comparison. One is the problem of identifying the underlying magnetic structure of microwave burst sources, which is implicit in any determination that reversal is being seen. Most active regions are bipolar in an east–west direction, and burst sources in general are often seen to be magnetically east–west bipolar, but less frequently than active regions. Secondly, many bursts seen to show multiple sources and highly complex structure, particularly at 1.5 GHz, and these are difficult to interpret.

We have inspected published VLA observations of microwave bursts, looking for events showing two sources in an east–west alignment, and rejecting events which are complex, north–south bipolar, or showing a single source. We have divided the resulting data arbitrarily into events within about  $30^\circ$  of CMP ('disk' events) and those more than  $30^\circ$  from CMP ('limb' events), and also divided them according to frequency (1.5, 5, or 15 GHz).

At 1.5 GHz, the observations show that both limb (Willson, 1984) and disk (Willson,



1984, 1985; Melozzi, Kundu, and Shevgaonkar, 1985) events are bipolar, and so no reversal is seen. At 5 GHz we find one example of a limb event with two sources of the same polarization (Melozzi, Kundu, and Shevgaonkar, 1985), one example of an event with two sources of opposite polarity at W 30 (Kundu, Schmahl, and Velusamy, 1982), and many complex examples which are unpolarized or difficult to interpret. At 15 GHz, both limb (Marsh *et al.*, 1981) and disk (Hoyng *et al.*, 1983; Shevgaonkar and Kundu, 1985) events seem to be bipolar.

The statistics of this survey are poor, but it shows no evidence that the polarization properties of microwave burst sources differ from those of SVC; specifically, 15 GHz bursts are bipolar everywhere, while 5 GHz bursts may show reversal at the limb (one marginal case in Melozzi, Kundu, and Shevgaonkar, 1985).

We can make a prediction about what differences should appear between SVC and burst polarization. The polarized component of SVC arises at low harmonics of  $f_B$ , whereas burst radiation is thought to be gyrosynchrotron radiation, at high harmonics. Thus at a given frequency, burst radiation should arise in a weaker magnetic field region than SVC. As we showed earlier, weaker source magnetic fields imply that  $f_i$  will be smaller in the QT region at a given frequency, and thus reversal is less likely. Thus if SVC at 15 GHz does show polarization inversion at the limb, then the apparent observation of bipolar burst sources at the limb at 15 GHz would be confirmation of this idea. In addition, at 1.5 GHz any observed burst source must lie above the optically-thick SVC layer, and thus the line of sight to such a source will have  $f > f_i$  as found in the previous section.

## 5. VLA Observations of Bipolar Noise Storm Continua

Noise storms are one of the most-studied solar radio emissions, yet they remain largely unexplained (Elgaroy, 1977; Kai, Melrose, and Suzuki, 1985). Noise storms at 327 MHz generally consist of a (non-flare) continuum component and a burst component. The continuum component (called ‘background continuum’ by Elgaroy, 1977) is broadband, generally covering a frequency range of about 70–400 MHz, but peaking at around 100–200 MHz, with variations on time scales of hours. The bursts (also known as type I bursts) are very narrow band, tend to occur in drifting chains of 10–20 MHz bandwidth, and have durations of the order of a second (or less at higher frequencies).

VLA observations of noise storms at 327 MHz offer much potential, because the VLA is capable of better sensitivity, better mapping ability on short time scales (including better dynamic range) and higher spatial resolution than previous observations. Since VLA observations at 327 MHz began in 1986, it has been found that noise storms are almost always present during the period of solar maximum, and that they are often so strong as to prevent study of other solar features at 327 MHz (Lang and Willson, 1987; Habbal, Ellman, and Gonzalez, 1989; Willson, Lang, and Liggett, 1990; Willson *et al.*, 1990). Exceptions may be found in Shevgaonkar, Kundu, and Jackson (1988), Lang, Willson, and Trotter (1988), and Lang and Willson (1989).

Here we will not discuss burst observations. The VLA is not ideal for studies of type I bursts for several reasons: its best practical time resolution has usually been too long to resolve most bursts, the chance of a type I chain (which is narrowband) occurring at 327 MHz is small, and identification of weak bursts as type I bursts, as opposed to one of the numerous other types of metric bursts (Güdel and Benz, 1988), is difficult (but possible with simultaneous spectral data, e.g., Willson *et al.*, 1990). In addition, most previous works on noise storms have concentrated on the burst emission, to the neglect of the continuum (although Elgaroy (1977) does contain a through summary of studies of the continuum).

We will focus on VLA observations of noise storm continuum, and specifically on bipolar sources. That bipolar noise storm sources are of great interest in the study of mode coupling was pointed out by Melrose (1973). The reason is as follows. Noise storm emission is thought to take place at the fundamental of the plasma frequency, since otherwise the high degrees of polarization observed are difficult to explain. Then

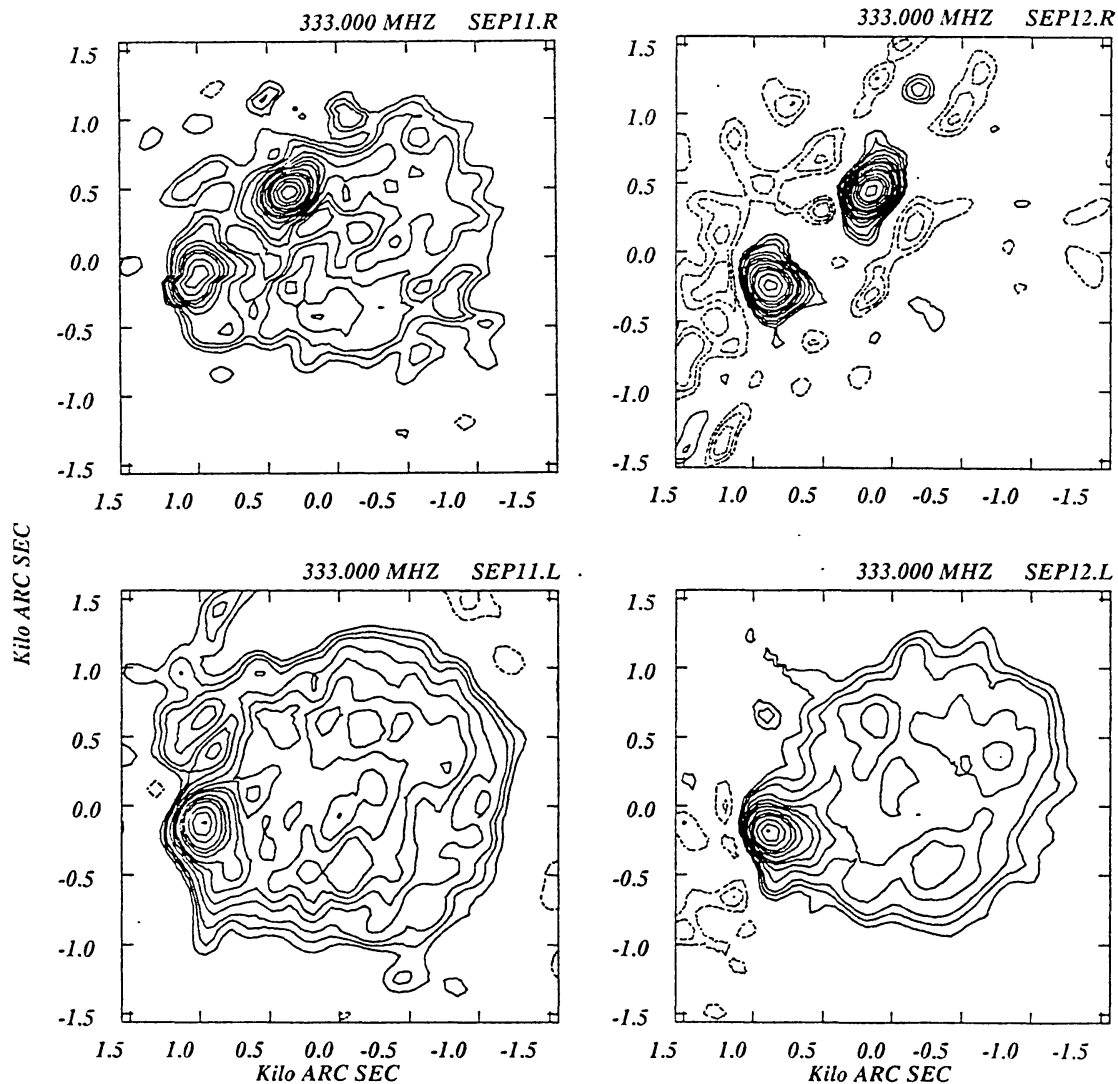


Fig. 2a.

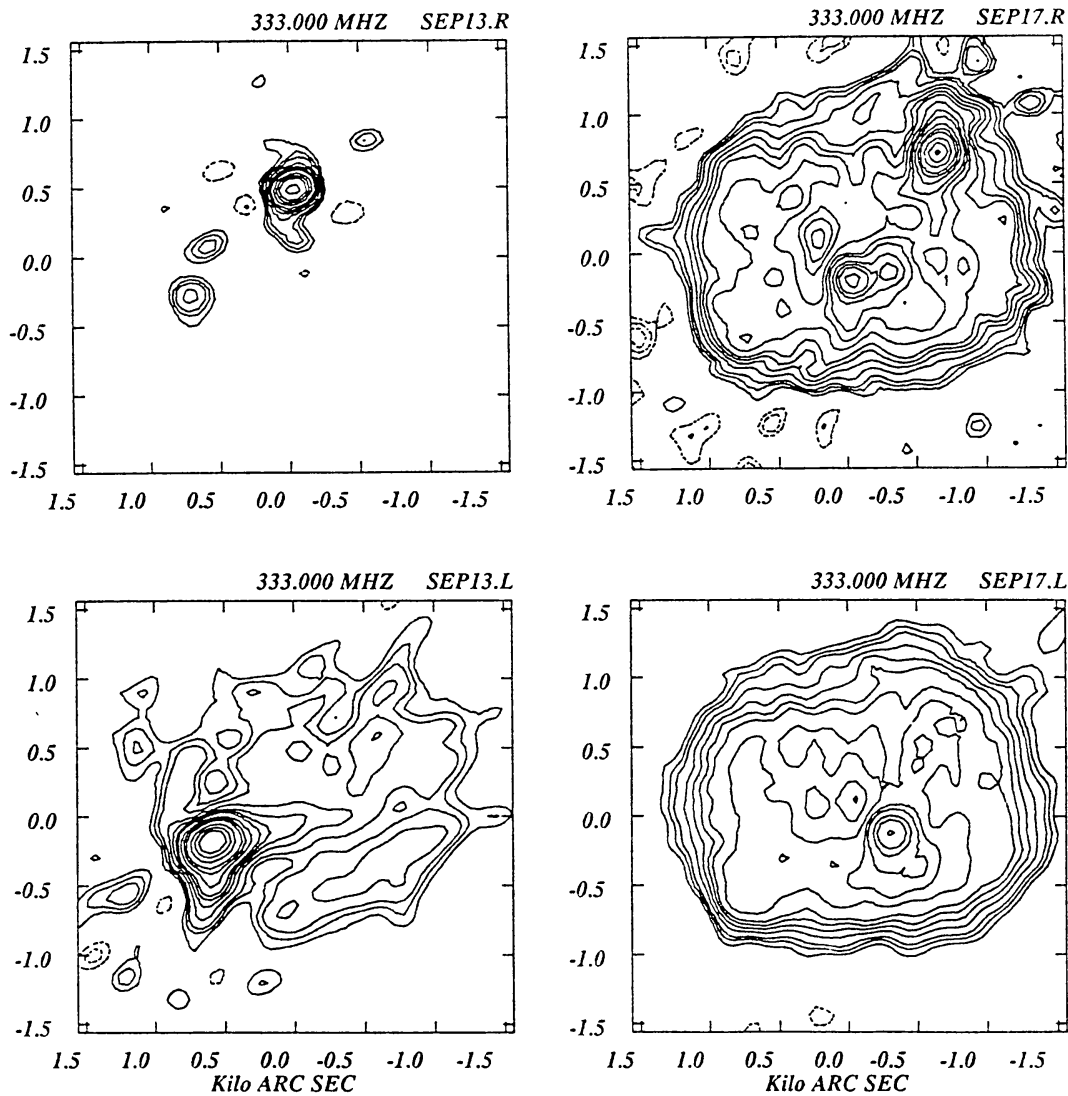


Fig. 2b.

Fig. 2. VLA maps of the Sun at 333 MHz on 1988 September 11, 12, 13, and 17. The upper four panels are the right circularly polarized flux, while the lower panels are the left circularly polarized flux. The maps are of variable quality due to the intrinsic variability of the background continuum; in particular, the quiet Sun is only reliably mapped in the last pair of maps on September 17, when both noise storms were weak; and the L maps are generally of better quality than the R maps. The contour levels are at  $2.5 \times 10^5$  K in the September 11 and 12 R maps,  $1.0 \times 10^5$  K in the September 11 and 12 L maps,  $2.0 \times 10^6$  K in the September 13 R map,  $2.0 \times 10^5$  K in the September 13 L map, and  $5.0 \times 10^4$  K in the September 17 R and L maps, with contours at the following multiples of the interval: -6, -4, -3, -2, 2, 3, 4, 6, 8, 10, 12, 16, 20, 24, 32, 40, 48, 64, 80, 96, 112, and 128. The beam size was approximately  $220'' \times 190''$  on all four days.

if radiation from a noise storm source near the limb encounters a QT layer in the active region the density there will be close to that in the source, i.e.,  $f \approx f_p$ . In this case Melrose shows that strong coupling is only possible at 100 MHz if  $B^3 L < 3 \times 10^7$  G<sup>3</sup> cm. For a typical scale length in the corona this requires  $B \ll 1$  G. Thus one would always expect to see polarization reversal from the limbward component of bipolar noise storms at 100 MHz, unless the radiation passes through a layer (such as a neutral layer) where

$B$  is very small. This probably requires refraction, since the neutral sheet is not generally expected to be at the same height as the closed magnetic flux tubes in which bipolar noise storms are thought to occur. Melrose (1973) also comments that if this is the correct explanation for bipolar noise storms at 100 MHz, one would expect that noise storms at higher frequencies might be unipolar since they arise lower in the corona and thus lines of sight to them should not pass through the neutral sheet. Suzuki and Sheridan

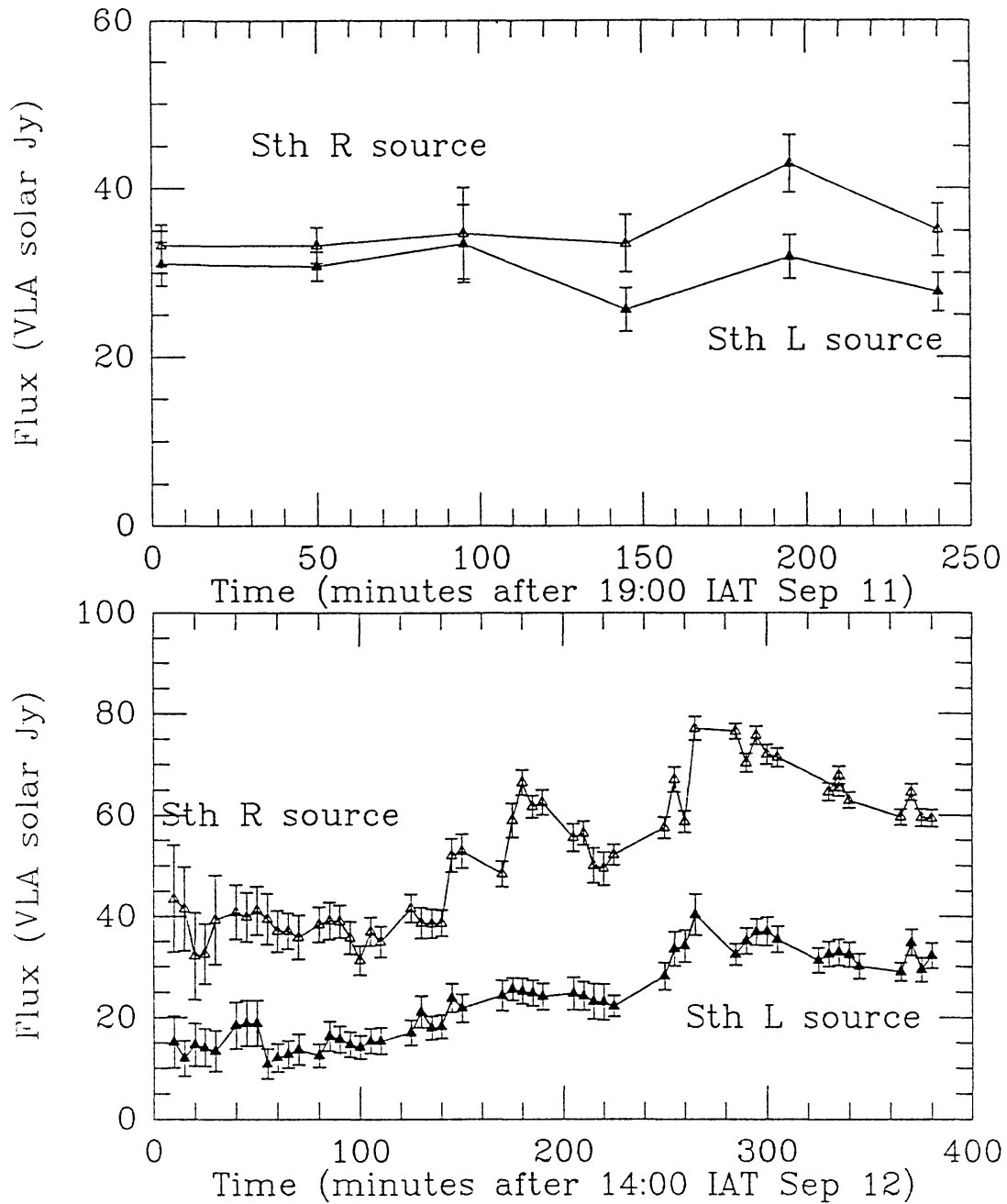


Fig. 3. Plots of the time variation of the peak flux in the two components of the bipolar noise storm above AR 5148 on September 11 (a) and September 12 (b). Units are in VLA solar Janskies (0.05 s.f.u.). The plots indicate that the two components show correlated variability. The R (trailing) component is stronger than the L (leading) component at all times.

(1980), using observed source heights, also find that at higher frequencies bipolar sources are only expected within a narrow region around CMP. From (2) with, say,  $f \approx 2.0f_p$  in the QT layer, it follows that at 327 MHz

$$Q \approx 0.03 B_{\text{gauss}}^{-3} \frac{10^{10} \text{ cm}}{L} \left( \frac{f}{327 \text{ MHz}} \right)^2 \quad (4)$$

(including the correction for refractive index effects pointed out by Melrose, 1974a) and again for plausible coronal parameters weak coupling will occur for limb sources at 327 MHz unless  $B \ll 1$  G. In order to discuss their relevance to mode coupling we will now summarize some of the properties of bipolar noise storms and present some new VLA observations.

Noise storms have been known to be often bipolar (Kai, 1970; Kai, Melrose, and Suzuki, 1985), but we cannot find statistics in the literature on the frequency of two-component as opposed to single-component continua (note that the burst component of noise storms is only very rarely bipolar, and individual bursts are apparently never bipolar). In Stewart's (1985) observations of noise storms at 160 MHz in 1976 and 1982, only about 5 out of 27 noise storms showed evidence for two sources, with all being bipolar. Although none of the previous VLA observations of noise storms report bipolar emission (Lang and Willson, 1987; Habbal, Ellman, and Gonzalez, 1989; Willson, Lang, and Liggett, 1990; Willson *et al.*, 1990), we have observed 5 separate noise storms at 327 MHz at the VLA of which 3 were clearly bipolar, one was a single source of close to 100% polarization, and the other was a limb source which was moderately polarized but cannot be easily categorized.

In Figure 2 we present 'D' configuration observations from 1988 September 11, 12, 13, and 17. On all four days the same pair of continuum noise storm sources is present: a unipolar (100% right-circularity polarized) source over AR 5142 in the north, and a bipolar source over AR 5148 in the south. The observations have low spatial resolution ( $\sim 3'$  beam), but they are adequate to measure the difference in the position of the L and R peaks in the northern source on September 12 and 13, and on September 17 the two components are clearly seen to be separated with the L peak leading in agreement with the leading spot hypothesis. On September 11 the southern noise storm was on the east limb, and it appears to be a very weakly polarized unipolar source. However, we believe that this is due to the fact that both parts of the bipole lie in the large beam on September 11, and the polarized fluxes from the two sources cancel. The peak brightness temperatures in the maps are as follows:  $1.4 \times 10^7$  K (September 11 R),  $4.9 \times 10^6$  K (September 11 L),  $1.7 \times 10^7$  K (September 12 R),  $4.9 \times 10^6$  K (September 12 L),  $7.1 \times 10^7$  K (September 13 R),  $1.3 \times 10^7$  K (September 13 L),  $5.0 \times 10^6$  K (September 17 R), and  $2.9 \times 10^6$  K (September 17 L). The beam size was approximately  $220'' \times 190''$  on all four days, and the sources are almost certainly unresolved. Adopting a true size of about  $40''$  (see below), we expect that the true peak brightness temperatures were more than an order of magnitude higher.

Only on September 17 are the noise storm sources weak enough for the quiet-Sun

component to be well-mapped. We note several things in the September 17 maps: the leading component of the southern storm is clearly seen to be not 100% polarized; the limb brightening can be seen; and the noise storm sources are all of low brightness temperature ( $\sim 3 \times 10^6$  K). In fact, if not for the observations on previous days these weak sources might not be recognized as noise storms (although at higher spatial resolution they might have appeared brighter).

We note that only when the noise storm over AR 5148 was at the east limb were the R and L sources observed to have the same flux: on all other days the R source was significantly stronger. This is curious because it is held that noise storms are generally unpolarized at the limb (Elgaroy, 1977). In our case we assume that the continuum is unpolarized because of the cancellation of the flux from oppositely polarized components within our large beam, but this explanation probably cannot be extended to other observations unless there is some reason why the two components of a bipolar storm always appear to have the same flux at the limb.

In the conventional model for noise storm continuum, nonthermal electrons are trapped in a large magnetic flux tube in the corona. The source of the nonthermal electrons is not well understood, but once present they can develop a loss-cone velocity anisotropy or a velocity distribution which can generate Langmuir waves, and these can then be converted into  $o$ -mode waves by one of a number of processes (Melrose, 1980b; Spicer, Benz, and Huba, 1981; Benz and Wentzel, 1981; Wentzel, 1986; Thejappa and Kundu, 1991). Implicit in this model is the idea that electrons are propagating backwards and forwards between the two ends of the loop. An obvious question regarding

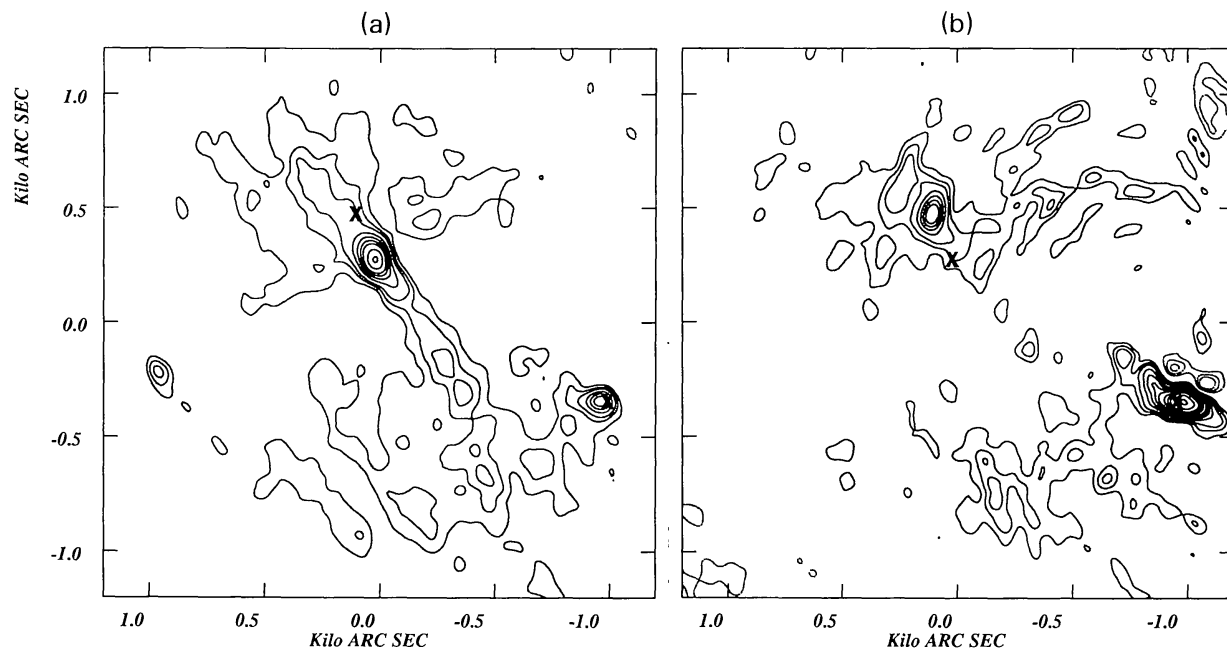


Fig. 4. 'BC'-hybrid configuration VLA maps of the Sun at 333 MHz on 1989 May 18 in right-circularly-polarized flux (a) and left-circularly-polarized flux (b). The maps have been rotated so that solar north is at the top. On each panel we have used crosses to mark the locations of the peaks in the other panel. The beam size is  $44'' \times 21''$ . The contour intervals are  $1.26 \times 10^6$  K in the R and L maps, with contours at the following multiples:  $-4, -3, -2, 2, 3, 4, 5, 6, 8, 10, 12, 14, 16, 20, 24, 32$ .

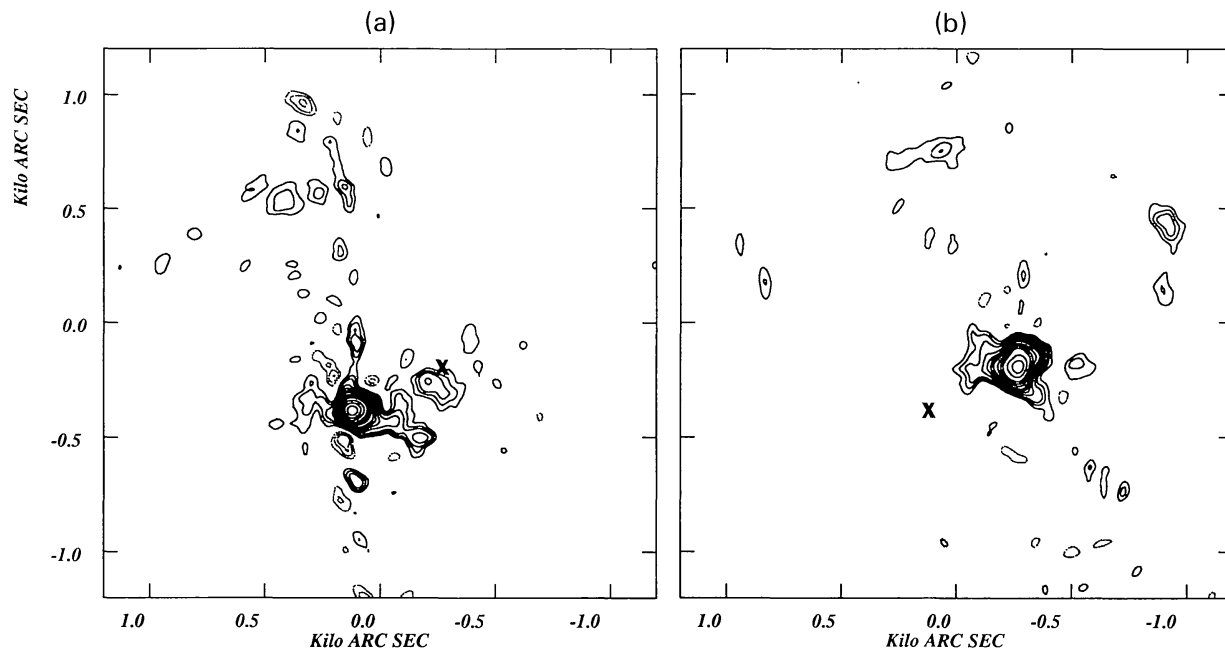


Fig. 5. 'BC'-hybrid configuration VLA maps of the Sun at 333 MHz on 1989 May 23 in right-circularly-polarized flux (a) and left-circularly-polarized flux (b). On each panel we have used crosses to mark the locations of the peaks in the other panel. The contour interval is  $2.42 \times 10^6$  K in both maps, with contours at the following multiples:  $-4, -3, -2, 2, 3, 4, 6, 8, 10, 12, 16, 20, 24, 28, 32, 40, 48, 64$ .

the continuum of bipolar noise storms is whether flux variations in the two sources are correlated, as one would expect in a loop model. We cannot find this point addressed in the literature, so in Figure 3 we plot the flux variations of the two components of the southern source as a function of time for September 11 and 12 (on September 13 the northern R source was too strong for us to measure fluxes in the southern R source reliably, while on September 17 all sources were too weak for time variability studies). It is clear that the variations in the two sources are correlated, consistent with the usual model in which the two sources lie in the legs of a single large loop (Piddington and Minnett, 1951). This figure also shows the level of variability typical of noise storm continua: changes of a factor of two in an hour can easily occur.

We obtained higher-spatial-resolution observations of noise storm continuum sources on 1989 May 18 (Figure 4) and May 23 (Figure 5). In these figures the left-hand panels are maps of right-circular-polarization, while the right-hand panels are maps of left-circular-polarization. On each panel we have used crosses to mark the locations of the peaks in the other polarization. In Figure 4 a bipolar noise storm is present in the northern hemisphere, oriented roughly north–south, while in the southern hemisphere another source lies close to the west limb. The south–western source is extended in the L map; in the R map only a single weak feature appears, which is well enclosed by the L source. This source may also be bipolar, with both components lying along the line of sight, or else it is not 100% polarized. A difficulty with VLA observations in this configuration ('B/C') is that limb smearing can be significant: thus, we tracked for rotation at disk center during these observations, but it moves about  $100''$  further than a limb source during the observation due to solar rotation. Thus the extended appear-

ance of the southern L source may be due to time-variability of the emission. The strongest peak in the southern L source is about 60% polarized. Bursts from this region during this day were found to range in polarization from 30% to 80% LH. The beam size is  $45'' \times 45''$ , with a peak brightness temperature of  $2.6 \times 10^7$  K in the R map and  $5.2 \times 10^7$  K in the L map. With high-resolution observations, Lang and Willson (1987) found that typical burst source sizes at 327 MHz are about  $40''$ , consistent with earlier observations (Elgaroy, 1977), and thus we believe that these brightness temperatures do not suffer from beam dilution. Some of the flux from the solar disk is visible in the R map; also, a weak new source can be seen at the east limb south of the equator in the R map.

In Figure 5 the prominent peaks in each polarization are continuum noise storm sources which were strong and variable on this day: peak brightness temperatures were  $1.3 \times 10^8$  K in the R map and  $1.1 \times 10^8$  K in the L map (beam size is  $56'' \times 45''$ ). A number of impulsive bursts were removed from the data before these maps were made. The impulsive bursts are easily seen in plots of flux versus time for a short baseline as

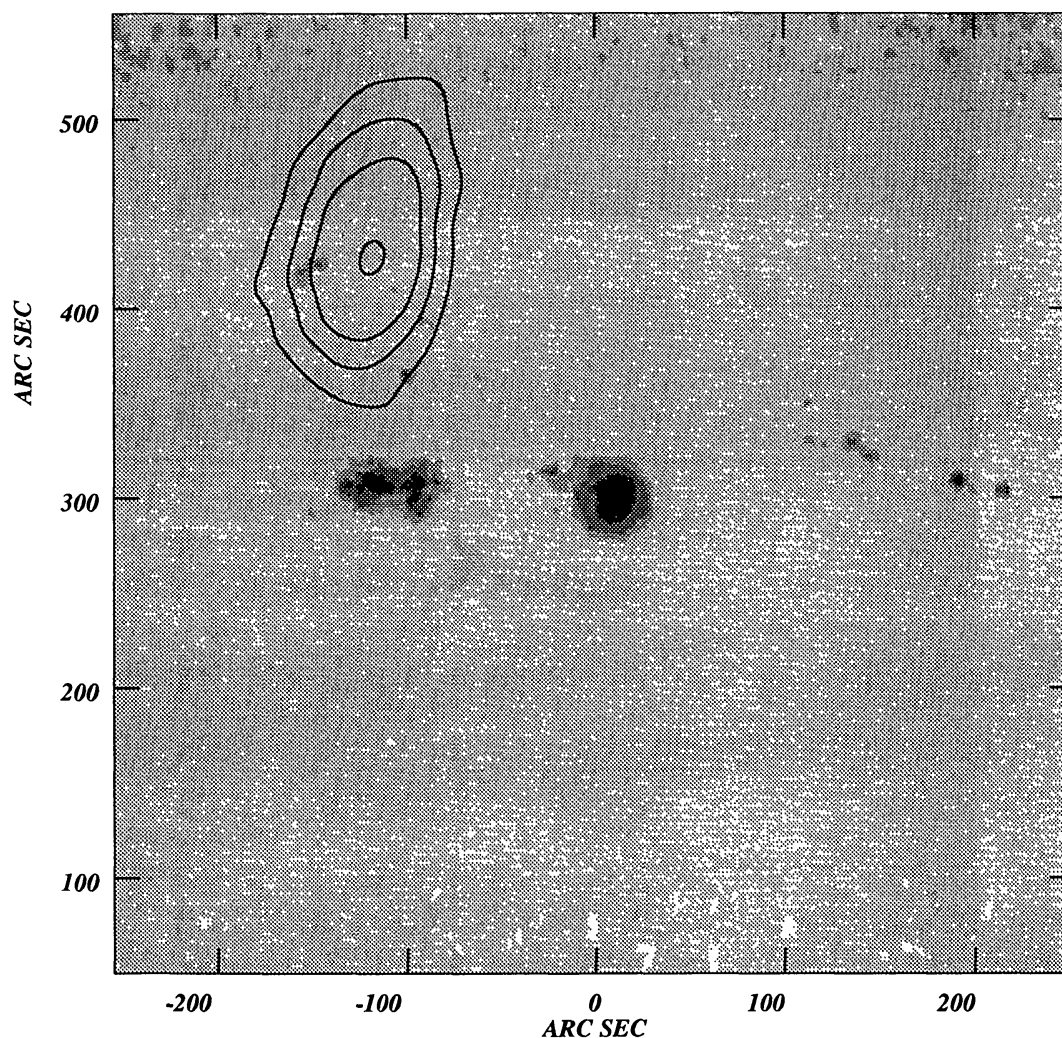


Fig. 6a.



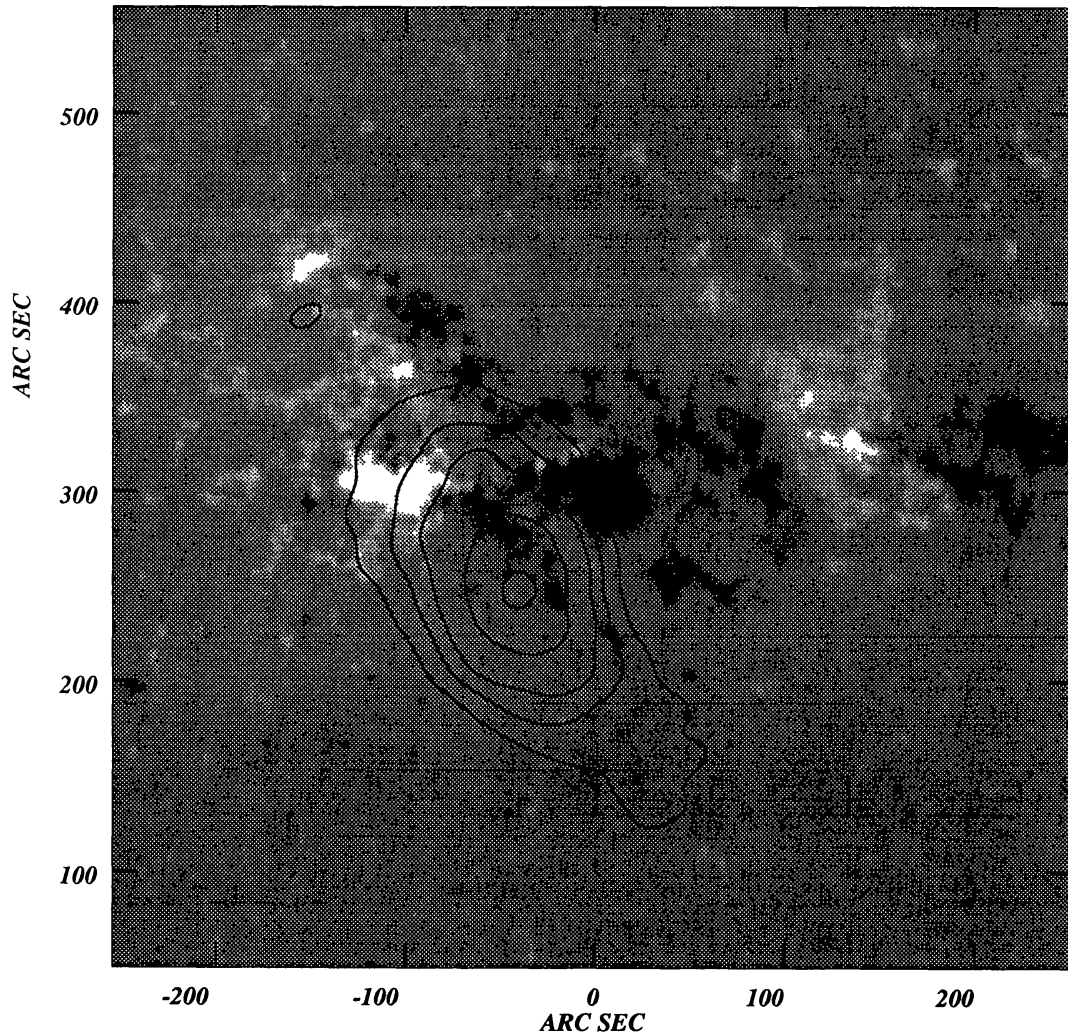


Fig. 6b.

Fig. 6. Overlaps of the bipolar radio source present in the north-east quadrant on 1989 May 18 on optical images from Kitt Peak National Observatory. (a) presents a radio image in left-circularly-polarized flux superposed on the KPNO brightness image, which shows the extent of umbra and penumbra within the active region. (b) presents a radio image in right-circularly-polarized flux superposed on the KPNO magnetogram. The radio images have been compressed by a factor of 1.1 radially towards the apparent center of the Sun in order to remove height projection effects.

features with time scales of seconds. By contrast, variations in the continuum level show up on time scales of about 10 minutes or longer. The variability of the continuum cannot be removed from the maps and it causes a number of artefacts to appear; in particular, the line of features running north-south from the main peak in the R map are artefacts. However, the weaker sources to the west of the peak in the R map appear to be real, and are due to a new source which appears in short-term maps during the second half of the day. In the L map probably only the main peak and the peak near the limb to the north-west are real.

In order to establish that the bipolar sources on 1989 May 18 and 23 are associated with regions of opposite polarity in the photosphere, we present overlays of the radio images on Kitt Peak images (courtesy of J. Harvey, KPNO) in Figures 6 (May 18) and

7 (May 23). In each figure there are two panels: one with the left-circularly-polarized radio image overlaid on the brightness image (which shows the extent of penumbra and umbra in the active regions), and the other with the right-circularly-polarized radio map overlaid on the magnetogram. The field of view is the same in each panel. The 0.33 GHz emission is generally thought to arise at a height of about  $1.1 R_{\odot}$ , which makes direct comparison of radio and optical locations difficult. In order to remove height projection effects in as unbiased a manner as possible, we have prepared these overlays by compressing the radio maps by a factor of 1.1 with respect to the apparent disk center. In the resulting images the two components of the bipole do straddle the photospheric neutral line in each case, and the components are all consistent with  $\sigma$ -mode polarity with respect to the underlying magnetic fields. There are no other nearby active regions outside the field of view shown which could be associated with the radio sources. We also note that in both cases the loop implied by the radio sources is twisted with respect to the magnetic axis on the underlying active region.

These observations that bipolar noise storms are at least as frequent in VLA observations as unipolar noise storms suggest that earlier low-resolution observations of noise storm continuum at lower frequencies, where source sizes are even larger, may have failed to detect such bipolarity as frequently because of inadequate resolution. One very curious result follows which has not received much attention. Since most noise storms

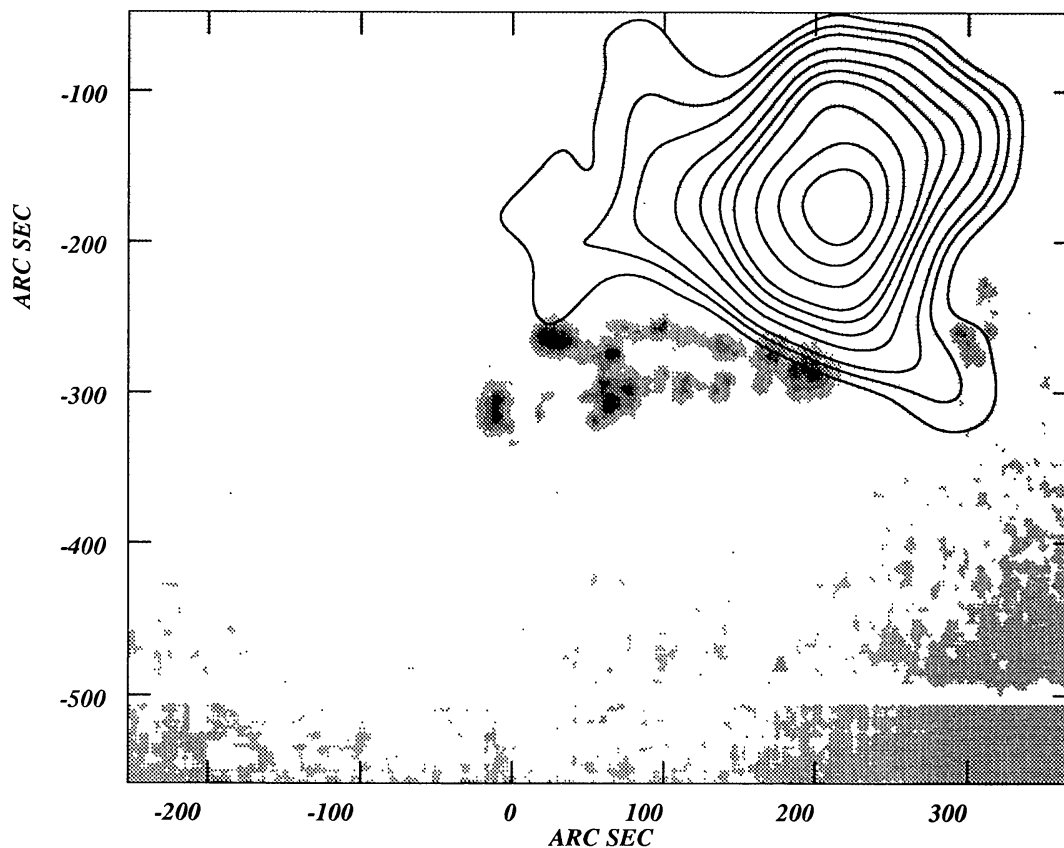


Fig. 7a.

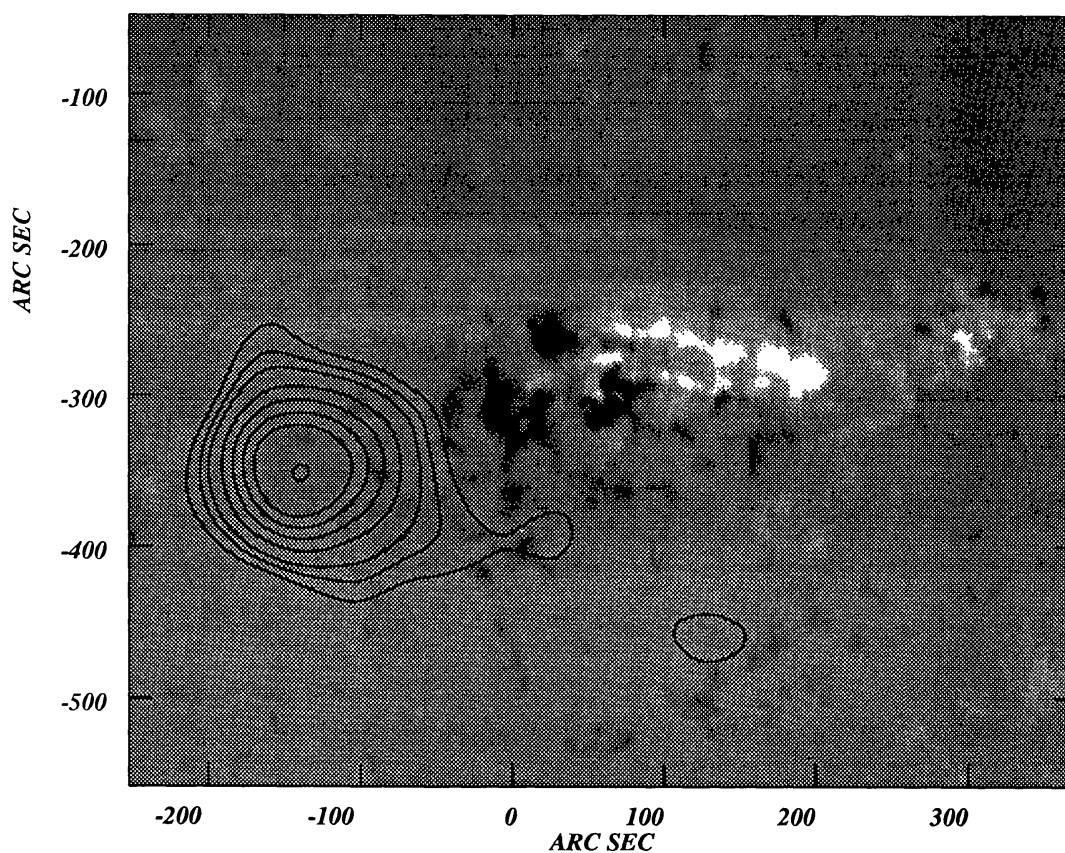


Fig. 7b.

Fig. 7. Overlays of the bipolar radio source present just below disk center on 1989 May 23 on optical images from Kitt Peak National Observatory. Figure 7a presents a radio image in left-circularly-polarized flux superposed on the KPNO brightness image. Figure 7b presents a radio image in right-circularly-polarized flux superposed on the KPNO magnetogram. The radio images have been compressed by a factor of 1.1 radially towards the apparent center of the Sun in order to remove height projection effects.

which do not appear to be bipolar are almost 100% polarized (Kai, Melrose, and Suzuki, 1985), at least on the disk, this implies that one component of the bipole is usually much weaker than the other. However, it is known that the polarization of unipolar noise storms generally conforms to the 'leading spot hypothesis': the polarization corresponds to  $\sigma$ -mode emission in the magnetic field of the leading spot in an active region. It follows that unipolar sources should be located over the leading spot, and one expects that in a bipolar source the leading component will be stronger. However, both in the case of AR 5148 and on May 23, and in half of the examples presented by Kai (1970), we find that the trailing component of a bipolar source is the stronger of the two. The discrepancy is weaker, however, when Stewart's (1985) results are taken into account: he found that in fact only 65% of all noise storms obey the leading spot rule. Further observations are required in order to establish whether the bipolar noise storm observations at 327 MHz are consistent with this figure.

What does this imply in the conventional model in which the two sources are in the legs of a single flux tube, and are due to nonthermal electrons in the loop? Suppose that the loop is asymmetric. Then the magnetic field in a region of given plasma density in

the trailing leg will usually be much weaker than in the same density layer in the leading leg. However, the nonthermal electrons on average follow the magnetic field lines, unless scattering is very strong, and if the nonthermal electrons are beamed then the number density of nonthermal electrons is then determined by magnetic flux conservation. Thus the number density of nonthermal electrons is likely to be higher in the stronger-field source in the leading leg of the flux tube. If the emission of plasma waves involves a nonlinear mechanism it would tend to strongly favor the stronger field source. We also offer a related explanation as the two individual bursts do not seem to be bipolar: we assume that the burst electrons originate in one leg of the loop, and that scattering in the burst source in that leg of the loop is so strong as to remove the free energy in the electrons before they propagate around to the other leg of the loop.

## 6. Mode Coupling and Noise Storms

The basic problem associated with mode coupling in noise storms is as follows: radiation from the limbward part of a bipolar source should pass through a QT region in the active region (i.e., a region where the component of  $\mathbf{B}$  along the line-of-sight changes sign). For typical coronal parameters (see Section 5), the QT region will be a weak-coupling layer and the polarization should reverse there. However, low-frequency observations (below 163 MHz) of two-component noise storms where positional information was available found that the two components were always observed to be oppositely polarized, i.e., the limbward component, if  $o$ -mode, does not show reversal (Suzuki, 1961; Kai, 1970; McLean and Sheridan, 1972; Kai and Sheridan, 1974). In addition, Stewart (1985, 1987) has shown that the heliospheric current sheet as projected onto the plane of the solar disk appears to separate the oppositely polarized components of bipolar noise storm sources. So far, we believe that VLA observations of noise storms at 327 MHz indicate that at the higher-frequency two-component noise storms are also bipolar, even at the limb. Thus the prediction by Melrose (1973) that higher-frequency observations of noise storms might show evidence for weak coupling, which the model of Suzuki and Sheridan (1980) is consistent with, are not confirmed: we believe that there continues to be no evidence for weak coupling in QT layers in observations of noise storms at metric wavelengths.

Essentially two explanations have been proposed. If the magnetic field in the QT region is always low, i.e., less than 0.1 G, or gradients in the QT layers are always very sharp, then the QT region will be a coupling layer (Melrose, 1973). Alternatively, if the component of  $\mathbf{B}$  along the line of sight reverses in a layer where  $B = 0$  instead of in a region where  $\theta = \pi/2$  then strong coupling occurs (Zheleznyakov and Zlotnik, 1978, 1988).

Both explanations require weak fields in any region where the component of  $\mathbf{B}$  along the line of sight changes sign. However, the second explanation is only sufficient if it is true that everywhere in the active region where  $\mathbf{k} \cdot \mathbf{B} = 0$ , it is also true that  $B = 0$ ; otherwise, the limbward radiation still encounters a QT region in which  $B \neq 0$ , and if it is a weak coupling layer then we will not see a bipolar source consistent with  $o$ -mode polarization in the source.

In order to have  $B = 0$  wherever  $\mathbf{k} \cdot \mathbf{B} = 0$  we require a simplified magnetic topology at the heights of noise storm radiation, such as the conventional helmet-streamer geometry which most models employ (e.g., Melrose, 1973), so that the component of  $\mathbf{B}$  along the line of sight reverses only within the active region. In the helmet streamer model the neutral sheet in which  $B = 0$  separates open field lines, and thus it must lie above the tallest closed field lines. But bipolar noise storms apparently lie on closed field lines, and if, as is common, noise storm emission extends down to a frequency of 50 MHz, by implication the lowest point of the neutral sheet must lie above the height corresponding to fundamental plasma emission at 50 MHz. Clearly then the 327 MHz source would arise at a much lower height than the lowest point on the neutral sheet. Thus lines of sight to the limbward source can only intersect such a neutral sheet if the region is not far from CMP, in which case we cannot explain bipolar noise storms near the limb. Alternatively we require refraction to increase the apparent height of the source by a large amount, as suggested by Melrose (1973). For bipolar sources near the limb we can also assume that all QT regions at low altitude are in fact neutral sheets, but amongst the closed field lines of the active region rather than between open field lines above the active region. We then require that the filling factor of lines of sight on which  $B = 0$  is almost unity.

On balance therefore we believe that it is unlikely that layers with  $B = 0$  can explain all the observations of bipolar noise storms, and therefore one still requires strong coupling in all QT layers encountered. Based on typical parameters (4) requires  $B < 0.2$  G for the 327 MHz QT layer (as discussed in Section 2 this value is only weakly sensitive to the values of  $n_e$  and  $L$ ), and this implies even lower values of  $B$  in the QT layers at lower frequencies (cf. limits of  $B < 1.5$  G for the 200 MHz QT layer discussed by Suzuki and Sheridan, 1980).

For sources near the limb the height of the QT layer will be similar to the height of the source, and then the magnetic fields in the two locations may be comparable. If the low value of the field strength found above is representative of the field strength in the noise storm source we can use it to discuss possible forms of fundamental plasma emission. Conventionally one argues that noise storm emission is highly polarized in the sense of the  $o$ -mode because, after the process of conversion from Langmuir waves, the transverse waves have frequencies below the  $x$ -mode cutoff at

$$f_x \approx f_p + \frac{1}{2}f_B \ll f_p. \quad (5)$$

Langmuir waves generated by electrons with a typical velocity  $v_b$  generally have a frequency

$$f \approx f_p + \frac{3v_e^2}{2v_b^2} f_p, \quad (6)$$

even when a loss-cone anisotropy is involved (Hewitt and Melrose, 1985). Suppose the frequency of the transverse wave is the same as that of the Langmuir wave: then the

transverse waves are only likely to be highly polarized if

$$\frac{f_B}{f_p} > \frac{3v_e^2}{v_b^2}. \quad (7)$$

For the solar corona at  $T_e = 2 \times 10^6$  K and with a plasma frequency of 327 MHz, this condition can be written as a minimum energy condition for the radiating electrons:  $E_{\text{keV}} > 60 B^{-1}$ . Thus emission by electrons of energies at least 300 keV is required as the source of 327 MHz emission in a region of  $B < 0.2$  G if it is highly polarized. These are much higher energies than are usually assumed. Correspondingly, any highly-polarized continuum brightness temperature below  $3 \times 10^9$  K is probably an optically thin incoherent emission process.

Now suppose that the Langmuir waves are converted to transverse waves by coalescence with low-frequency ion-sound waves (Melrose, 1980b). The typical frequency of a coalescing ion-sound wave is  $f \approx kv_s$  where  $v_s = (T_e/m_i)^{1/2}$  is the ion sound speed at  $k \approx f_p/v_b$ . This gives us the condition

$$\frac{f_B}{f_p} > \frac{3v_e^2}{v_b^2} + 2 \left( \frac{m_e}{m_i} \right)^{1/2} \frac{v_e}{v_b}. \quad (8)$$

If  $B = 1.0$  G in the source, this condition becomes  $E > 84$  keV; if  $B = 0.2$  G in the source, then we require  $E > 560$  keV. Again these constraints on the radiating energy lead to lower limits which seem too high, and we conclude that the magnetic field must be much stronger in the noise storm source than in any strong coupling QT layer along the line of sight if the two components of a bipolar noise storm are highly polarized, as our observations show.

Weak coupling at meter wavelengths has been reported by Benz, Urbarz, and Zlobec (1979) in observations of U bursts at 237 MHz (thought to be type-III-like plasma emission by electron streams on closed, rather than open, field lines; Labrum and Stewart, 1970). They found that the two 'legs' of the U burst, which by implication lie in opposite legs of a magnetic flux tube, were generally of the same polarization. However, as is usual in type III bursts, the degree of polarization was small in all cases. Observations of U bursts at lower frequencies do not show weak coupling, i.e., the two legs show opposite circular polarizations at 80 MHz (Sheridan, McLean, and Smerd, 1973; Suzuki, 1978; Suzuki and Sheridan, 1978). Suzuki and Sheridan (1980) argue that in fact this trend is consistent with models for the corona, but the result implies that magnetic fields in QT layers for U bursts are generally stronger than they are for noise storms at the same frequency, whereas the low degree of polarization suggests that the magnetic field is larger in the U burst source than in noise storms. This combination of circumstances seems difficult to understand.

## 7. Summary

We have reviewed the present knowledge of mode coupling in solar radiophysics, with emphasis on recent high-spatial-resolution observations. The main conclusions are as follows:

(i) Polarization inversion (i.e., weak mode coupling) is seen in SVC sources near the limb at 5 GHz and probably at higher frequencies also. However, it is not seen at 1.5 GHz. While this is in apparent contradiction to the simple notion that there exists a critical frequency below which polarization inversion should be seen, in fact it is not inconsistent with current models for SVC at different frequencies. In particular, 5 GHz emission is gyroresonance emission from regions of 600 G field strength, while 1.5 GHz emission is thermal bremsstrahlung emission in regions with 20 G fields. Since magnetic field strength is the main factor in determining whether weak or strong coupling will be seen in QT layers, the factor of 30 difference can easily account for the presence of strong coupling at low frequencies.

(ii) We expect that microwave bursts at a given frequency should be less likely to show polarization than SVC at the same frequency. However, present observations are inadequate to detect such an effect, and presently show no discernible difference from the properties of SVC.

(iii) We have presented new VLA observations of bipolar noise storms at 327 MHz, and demonstrated that time variability in the continuum emission from the two components is correlated, in agreement with a model in which the two components are on opposite legs of a large loop structure. Bipolar noise storms seem to be almost as common as single-component noise storms at 327 MHz, at least with the VLA's good sensitivity. One interesting observation is that frequently the trailing component of a bipolar noise storm is the stronger, whereas the leading spot hypothesis, based on observations of mostly single-component noise storms, would suggest that the leading component should usually be stronger.

(iv) However, there is no evidence for the presence of weak coupling in noise storm sources at 327 MHz near the limb, in contradiction to the speculation by Melrose (1973) and the modelling of Suzuki and Sheridan (1980). The evidence suggests that mode coupling is strong at all QT layers in the corona. This requires weak magnetic fields in the corona at the heights of noise storm sources, and we are able to place even stronger constraints than previously possible using the higher frequency observations. A maximum field strength of about 0.15 G is implied for the 327 MHz QT layer, with by implication even lower field strength at lower frequencies.

Thus reconciliation of noise storm observations with the predictions of mode coupling theory continues to be a problem, in that it seems to require much weaker coronal magnetic fields than we expect (e.g., Hoeksema and Scherrer, 1986). One aspect of this problem is that field strengths of 20 G are deduced in the 1.5 GHz SVC sources, but typical densities in those sources are assumed to be  $1\text{--}5 \times 10^9 \text{ cm}^{-3}$  (Dulk and Gary, 1983; Gopalswamy, White, and Kundu, 1991). The density in the 327 MHz noise storm source is  $1.3 \times 10^9 \text{ cm}^{-3}$  (assuming fundamental plasma emission). Thus as density

drops by a factor of only 2 or 3, the magnetic field strength drops by two orders of magnitude. The numbers are slightly better if we assume that the density and magnetic field strength are higher in the noise storm source than in the surrounding corona, but still appear daunting. Clearly this invites an explanation other than those discussed here.

### Acknowledgements

We thank M. Pick of Meudon Observatory for supplying us with Nançay radioheliograph data and J. Harvey of Kitt Peak National Observatory for providing digitized Kitt Peak images. We thank N. Gopalswamy and E. Schmahl for their comments. This work was supported by NSF grant ATM-90-19893 and NASA grant NAG-W-1541.

### References

- Abramov-Maksimov, V. E. and Gelfreikh, G. B.: 1983, *Soviet Astron. Letters* **9**, 132.
- Alissandrakis, C. E.: 1986, *Solar Phys.* **104**, 207.
- Alissandrakis, C. E. and Kundu, M. R.: 1984, *Astron. Astrophys.* **139**, 271.
- Alissandrakis, C. E. and Preka-Papadema, P.: 1984, *Astron. Astrophys.* **139**, 507.
- Bandiera, R.: 1982, *Astron. Astrophys.* **112**, 52.
- Bastian T. S.: 1987, Ph. D. Thesis, University of Colorado, unpublished.
- Benz, A. O. and Wentzel, D. G.: 1981, *Astron. Astrophys.* **94**, 100.
- Benz, A. O., Urbarz, H., and Zlobec, P.: 1979, *Astron. Astrophys.* **79**, 216.
- Cohen, M. H.: 1960, *Astrophys. J.* **131**, 664.
- Dulk, G. A. and Gary, D. E.: 1983, *Astron. Astrophys.* **124**, 103.
- Elgaroy, O.: 1977, *Solar Noise Storms*, Pergamon Press, Oxford.
- Ginzburg, V. L. and Zheleznyakov, V. V.: 1961, *Soviet Astron.* **5**, 1.
- Gopalswamy, N., White, S. M., and Kundu, M. R.: 1991, *Astrophys. J.* **379**, 366.
- Güdel, M. and Benz, A. O.: 1988, *Astron. Astrophys. Suppl. Ser.* **75**, 243.
- Habal, S. R., Ellman, N. E., and Gonzalez, R.: 1989, *Astrophys. J.* **342**, 594.
- Hewitt, R. G. and Melrose, D. B.: 1985, *Solar Phys.* **96**, 157.
- Hoeksema, J. T. and Scherrer, P. H.: 1986, *Solar Phys.* **105**, 205.
- Hoyng, P., Marsh, K. A., Zirin, H., and Dennis, B. R.: 1983, *Astrophys. J.* **268**, 865.
- Kai, K.: 1970, *Solar Phys.* **11**, 456.
- Kai, K. and Sheridan, K. V.: 1974, *Solar Phys.* **35**, 181.
- Kai, K., Melrose, D. B., and Suzuki, S.: 1985, in D. J. MacLean and N. R. Labrum (eds.), *Solar Radiophysics*, Cambridge University Press, Cambridge, p. 415.
- Kakinuma, T. and Swarup, G.: 1962, *Astrophys. J.* **136**, 975.
- Kundu, M. R.: 1959, *Ann. Astrophys.* **22**, 1.
- Kundu, M. R. and Alissandrakis, C. E.: 1984, *Solar Phys.* **94**, 249.
- Kundu, M. R., Schmahl, E. J., and Velusamy, T.: 1982, *Astrophys. J.* **253**, 963.
- Kundu, M. R., Alissandrakis, C. E., Bregman, J. D., and Hin, A.: 1977, *Astrophys. J.* **213**, 278.
- Labrum, N. R. and Stewart, R. T.: 1970, *Proc. Astron. Soc. Australia* **1**, 316.
- Lang, K. R. and Willson, R. F.: 1987, *Astrophys. J.* **319**, 514.
- Lang, K. R. and Willson, R. F.: 1989, *Astrophys. J.* **344**, L73.
- Lang, K. R., Willson, R. F., and Trotter, G.: 1988, *Astron. Astrophys.* **199**, 325.
- Marsh, K. A., Hurford, G. J., Zirin, H., Dulk, G. A., Dennis, B. R., Frost, K. J., and Orwig, L. E.: 1981, *Astrophys. J.* **251**, 797.
- McLean, D. J. and Sheridan, K. V.: 1972, *Solar Phys.* **26**, 176.
- Melozzi, M., Kundu, M. R., and Shevgaonkar, R. K.: 1985, *Solar Phys.* **97**, 345.
- Melrose, D. B.: 1973, *Proc. Astron. Australia* **2**, 208.
- Melrose, D. B.: 1974a, *Australian J. Phys.* **27**, 31.
- Melrose, D. B.: 1974b, *Australian J. Phys.* **27**, 43.



- Melrose, D. B.: 1980a, *Plasma Astrophysics*, Gordon and Breach, New York.
- Melrose, D. B.: 1980b, *Solar Phys.* **67**, 357.
- Peterova, N. G. and Akhmedov, S. B.: 1974, *Soviet Astron.* **17**, 768.
- Piddington, J. H. and Minnett, H. C.: 1951, *Australian J. Sci. Res.* **A4**, 131.
- Preka-Papadema, P. and Alissandrakis, C. E.: 1988, *Astron. Astrophys.* **191**, 365.
- Ramaty, R.: 1969, *Astrophys. J.* **158**, 753.
- Sheridan, K. V., McLean, D. J., and Smerd, S. F.: 1973, *Astrophys. Letters* **15**, 139.
- Shevgaonkar, R. K. and Kundu, M. R.: 1985, *Astrophys. J.* **292**, 733.
- Shevgaonkar, R. K., Kundu, M. R., and Jackson, P. D.: 1988, *Astrophys. J.* **329**, 982.
- Spicer, S. D., Benz, A. O., and Huba, J. D.: 1981, *Astron. Astrophys.* **105**, 221.
- Stewart, R. T.: 1985, *Solar Phys.* **96**, 381.
- Stewart, R. T.: 1987, *Solar Phys.* **109**, 139.
- Suzuki, S.: 1961, *Ann. Tokyo Astron. Obs. Ser.* **2**, 75.
- Suzuki, S.: 1978, *Solar Phys.* **57**, 415.
- Suzuki, S. and Sheridan, K. V.: 1978, *Radiophys. Quant. Electron.* **20**, 989.
- Suzuki, S. and Sheridan, K. V.: 1980, *Proc. Astron. Soc. Australia* **4**, 56.
- Tanaka, H. and Kakinuma, T.: 1959, in R. N. Bracewell (ed.), *Paris Symposium on Radio Astronomy*, Stanford University Press, Stanford, p. 215.
- Thejappa, G. and Kundu, M. R.: 1991, *Solar Phys.* **132**, 155.
- Wentzel, D. G.: 1986, *Solar Phys.* **103**, 141.
- White, S. M., Kundu, M. R., and Gopalswamy, N.: 1991a, *Astrophys. J.* (in press).
- White, S. M., Kundu, M. R., and Gopalswamy, N.: 1991b, *Astrophys. J.* **366**, L43.
- Willson, R. F.: 1984, *Solar Phys.* **92**, 189.
- Willson, R. F.: 1985, *Astrophys. J.* **298**, 911.
- Willson, R. F., Lang, K. R., and Liggett, M.: 1990, *Astrophys. J.* **350**, 856.
- Willson, R. F., Klein, K. L., Kerdraon, A., Lang, K. R., and Trotter, G.: 1990, *Astrophys. J.* **357**, 662.
- Zheleznyakov, V. V.: 1962, *Soviet Astron. AJ* **6**, 3.
- Zheleznyakov, V. V.: 1977, *Electromagnetic Waves in Cosmic Plasma: Generation and Propagation*, Nauka, Moscow.
- Zheleznyakov, V. V. and Zlotnik, E. Y.: 1964, *Soviet Astron.* **7**, 485.
- Zheleznyakov, V. V. and Zlotnik, E. Y.: 1978, *Radiophys. Quant. Electron.* **20**, 997.
- Zheleznyakov, V. V. and Zlotnik, E. Y.: 1988, *Soviet Astron. Letters* **14**, 73.
- Zheleznyakov, V. V., Kocharovskii, V. V., and Kocharovskii, V. V.: 1984, *Soviet Phys. Usp.* **26**, 877.